Spatiotemporal variations of seismicity before major earthquakes in the Japanese area and their relation with the epicentral locations

Nicholas V. Sarlis[a], Efthimios S. Skordas[a], Panayiotis A. Varotsos[a], Toshiyasu Nagao[b], Masashi Kamogawa[c], and Seiya Uyeda[d,1]

[a]Solid State Section and Solid Earth Physics Institute, Physics Department, University of Athens, Zografou 157 84, Athens, Greece; [b]Earthquake Prediction Research Center, Institute of Oceanic Research and Development, Tokai University, Shizuoka 424-0902, Japan; [c]Department of Physics, Tokyo Gakugei University, Koganei-shi 184-8501, Japan; and [d]Section II, Division 4, Japan Academy, Tokyo, 110-0007, Japan

Contributed by Seiya Uyeda, December 3, 2014 (sent for review November 25, 2014)

Using the Japan Meteorological Agency earthquake catalog, we investigate the seismicity variations before major earthquakes in the Japanese region. We apply natural time, the new time frame, for calculating the fluctuations, termed β, of a certain parameter of seismicity, termed κ_1. In an earlier study, we found that β calculated for the entire Japanese region showed a minimum a few months before the shallow major earthquakes (magnitude larger than 7.6) that occurred in the region during the period from 1 January 1984 to 11 March 2011. In this study, by dividing the Japanese region into small areas, we carry out the β calculation on them. It was found that some small areas show β minimum almost simultaneously with the large area and such small areas clustered within a few hundred kilometers from the actual epicenter of the related main shocks. These results suggest that the present approach may help estimation of the epicentral location of forthcoming major earthquakes.

criticality | seismic electric signals | natural time analysis

In this study, we investigate the evolution of seismicity shortly before main shocks in the Japanese region, $N_{25}^{46}E_{125}^{148}$, using Japan Meteorological Agency (JMA) earthquake catalog as in ref 1. For this, we adopted the new time frame called natural time since our previous works using this time frame made the lead time of prediction as short as a few days (see below). For a time series comprising N earthquakes (EQs), the natural time χ_k is defined as $\chi_k = k/N$, where k means the k^{th} EQ with energy Q_k (Fig. 1). Thus, the raw data for our investigation, to be read from the earthquake catalog, are $\chi_k = k/N$ and $p_k = Q_k/\sum_{n=1}^{N} Q_n$, where p_k is the normalized energy. In natural time, we are interested in the order and energy of events but not in the time intervals between events.

We first calculate a parameter called κ_1, which is defined as follows (2, 3), from the catalog.

$$\kappa_1 = \sum_{k=1}^{N} p_k \chi_k^2 - \left(\sum_{k=1}^{N} p_k \chi_k\right)^2 = \langle \chi^2 \rangle - \langle \chi \rangle^2. \quad [1]$$

We start the calculation of κ_1 at the time of initiation of Seismic Electric Signals (SES), the transient changes of the electric field of Earth that have long been successfully used for short-term EQ prediction (4, 5). The area to suffer a main shock is estimated on the basis of the selectivity map (4, 5) of the station that recorded the corresponding SES. Thus, we now have an area in which we count the small EQs of magnitude greater than or equal to a certain magnitude threshold that occur after the initiation of the SES. We then form time series of seismic events in natural time for this area each time a small EQ occurs, in other words, when the number of the events increases by one. The κ_1 value for each time series is computed for the pairs (χ_k, p_k) by considering that χ_k is "rescaled" to $\chi_k = k/(N+1)$ together with rescaling $p_k = Q_k/\sum_{n=1}^{N+1} Q_n$ upon the occurrence of any additional event in the area. The resulting number of thus computed κ_1 values is usually of the order 10^2 to 10^3 depending, of course, on the magnitude threshold adopted for the events that occurred after the SES initiation until the main shock occurrence. When we followed this procedure, it was found empirically that the values of κ_1 converge to 0.07 a few days before main shocks. Thus, by using the date of convergence to 0.07 for prediction, the lead times, which were a few months to a few weeks or so by SES data alone, were made, although empirically, as short as a few days (6, 7). In fact, the prominent seismic swarm activity in 2000 in the Izu Island region, Japan, was preceded by a pronounced SES activity 2 mo before it, and the approach of κ_1 to 0.07 was found a few days before the swarm onset (8). However, when SES data are not available, which is usually the case, it is not possible to follow the above procedure. To cope with this difficulty, in the previous work (1), we investigated the time change of the fluctuation of the κ_1 values during a few preseismic months for each EQ (which we call target EQ) over the large area $N_{25}^{46}E_{125}^{148}$ (Fig. 2*A*) for the period from 1 January 1984 to 11 March 2011, the day of *M*9.0 Tohoku EQ. Setting a threshold $M_{JMA} = 3.5$ to assure data completeness of JMA catalog, we were left with 47,204 EQs in the concerned period of about 326 mo: ∼150 EQs per month. For calculating the β values, we chose 200 EQs before target EQs to cover the seismicity in almost one and a half months.

To obtain the fluctuation β of κ_1, we need many values of κ_1 for each target EQ. For this purpose, we first took an excerpt comprised of W successive EQs just before a target EQ from the seismic catalog. The number W was chosen to cover a period of a few months. For this excerpt, we form its subexcerpts $S_j = \{Q_{j+k-1}\}_{k=1,2,\ldots,N}$ of consecutive $N = 6$ EQs (since at least

Significance

It was recently found that a few months before major earthquakes, the seismicity in the entire Japanese region exhibits a characteristic change. This change, however, can be identified when seismic data are analyzed in a new time domain termed "natural time." By dividing the Japanese region into small areas, we find that some small areas show the characteristic change almost simultaneously with the large area and such small areas are clustered within a few hundred kilometers from the actual epicenter of the related major earthquake. This phenomenon may serve for forecasting the epicenter of a future major earthquake.

Author contributions: N.V.S. and P.A.V. designed research; N.V.S., E.S.S., P.A.V., T.N., M.K., and S.U. performed research; N.V.S. and E.S.S. analyzed data; and N.V.S., E.S.S., P.A.V., T.N., M.K., and S.U. wrote the paper.

The authors declare no conflict of interest.

See Commentary on page 944.

[1]To whom correspondence should be addressed. Email: suyeda@st.rim.or.jp.

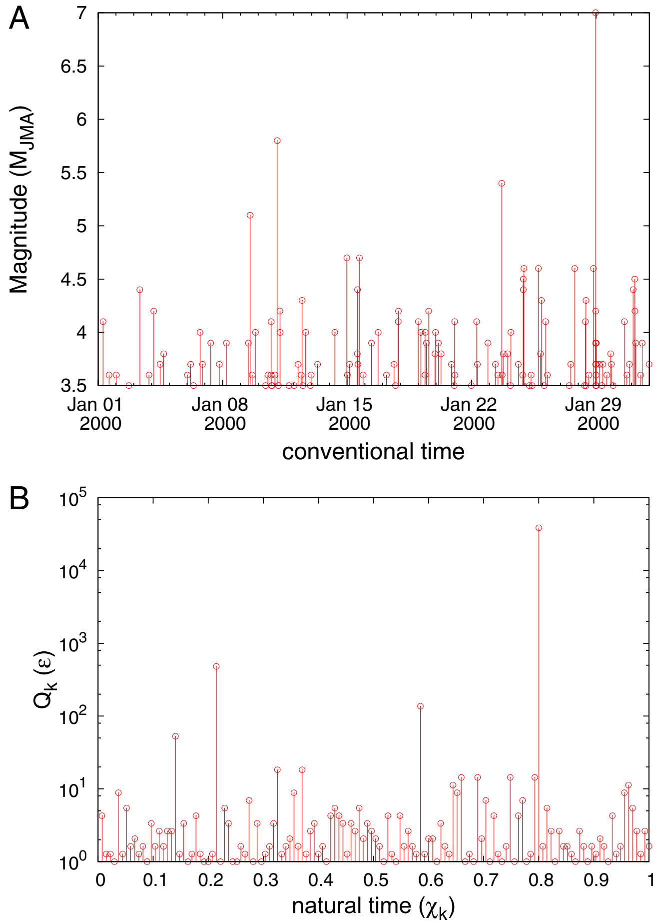

Fig. 1. EQ sequence in (*A*) conventional time and (*B*) natural time. In *B*, Q_k is given in units of the energy ε corresponding to a $3.5M_{JMA}$ EQ.

six EQs are needed (2) for obtaining reliable κ_1) of energy Q_{j+k-1} and natural time $\chi_k = k/N$ each. Further, $p_k = Q_{j+k-1}/\sum_{k=1}^{N} Q_{j+k-1}$, and by sliding S_j over the excerpt of W EQs, $j = 1, 2, \ldots, W - N + 1$ (= W – 5), we calculate κ_1 using Eq. **1** for each j. We repeat this calculation for $N = 7, 8, \ldots, W$, thus obtaining an ensemble of [(W – 4)(W – 5)]/2 (= 1 + 2 +…+ W – 5) κ_1 values. Then, we compute the average $\mu(\kappa_1)$ and the SD $\sigma(\kappa_1)$ of thus obtained ensemble of [(W – 4)(W – 5)]/2 κ_1 values. The variability β of κ_1 for this excerpt W is defined to be $\beta \equiv \sigma(\kappa_1)/\mu(\kappa_1)$ and is assigned to the $(W + 1)^{\text{th}}$ EQ, i.e., the target EQ.

The time evolution of the β value can be pursued by sliding the excerpt through the EQ catalog. Namely, through the same process as above, β values assigned to $(W + 2)^{\text{th}}$, $(W + 3)^{\text{th}}$, … EQs in the catalog can be obtained.

We found in ref. 1 that the fluctuation β of κ_1 values exhibited minimum a few months before all of the six shallow EQs of magnitude larger than 7.6 that occurred in the study period. A minimum of $\beta \equiv \sigma(\kappa_1)/\mu(\kappa_1)$ means large average and/or small deviation of κ_1 values (e.g., see ref. 9).

In the present work, we calculate the β values for small areas before the six large EQs, which showed β minima of the large area.

The Relation Between β Minimum of Small Areas and the Epicentral Area of a Forthcoming Main Shock

The way to calculate the β value in this work is the same as in ref. 1, except we worked (i) not on every EQ but on the six major EQs and (ii) on a large number of small areas instead of one large area. For consistency, we chose W also as the number of EQs that on average occur in each small area within one and a half months to be used for calculating the β in small areas (see Fig. 2 *B* and *C*). The data source is the same JMA seismic catalog. For this purpose, we set circular areas with radius R = 250 km of

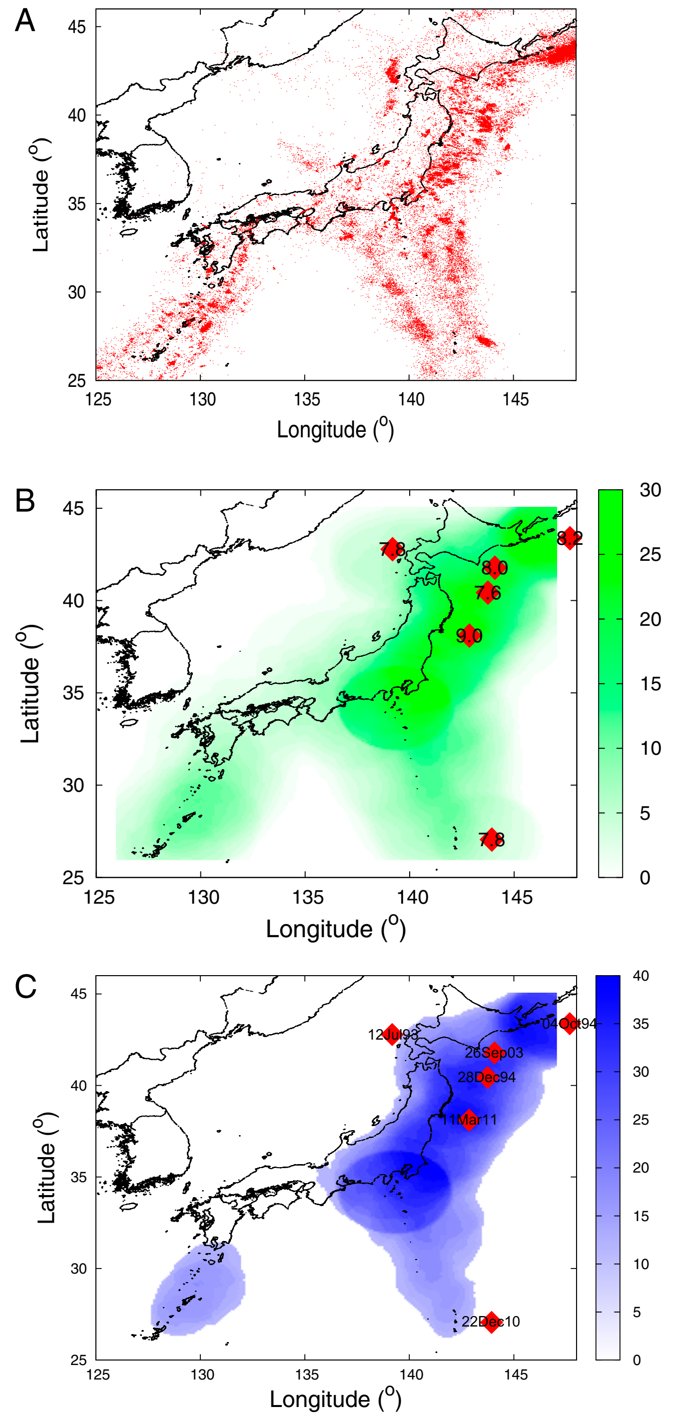

Fig. 2. (*A*) The 47,204 EQs with $M_{JMA} \geq 3.5$ that occurred during the period of our study. (*B*) Contours of the number of EQs per month within R = 250 km. Solid diamonds show the epicenters of six shallow EQs investigated in this study. (*C*) Contours of the natural time window W used in each of the 12,476 areas of radius R = 250 km with offset 0.1° from one another that have at least eight EQs per month.

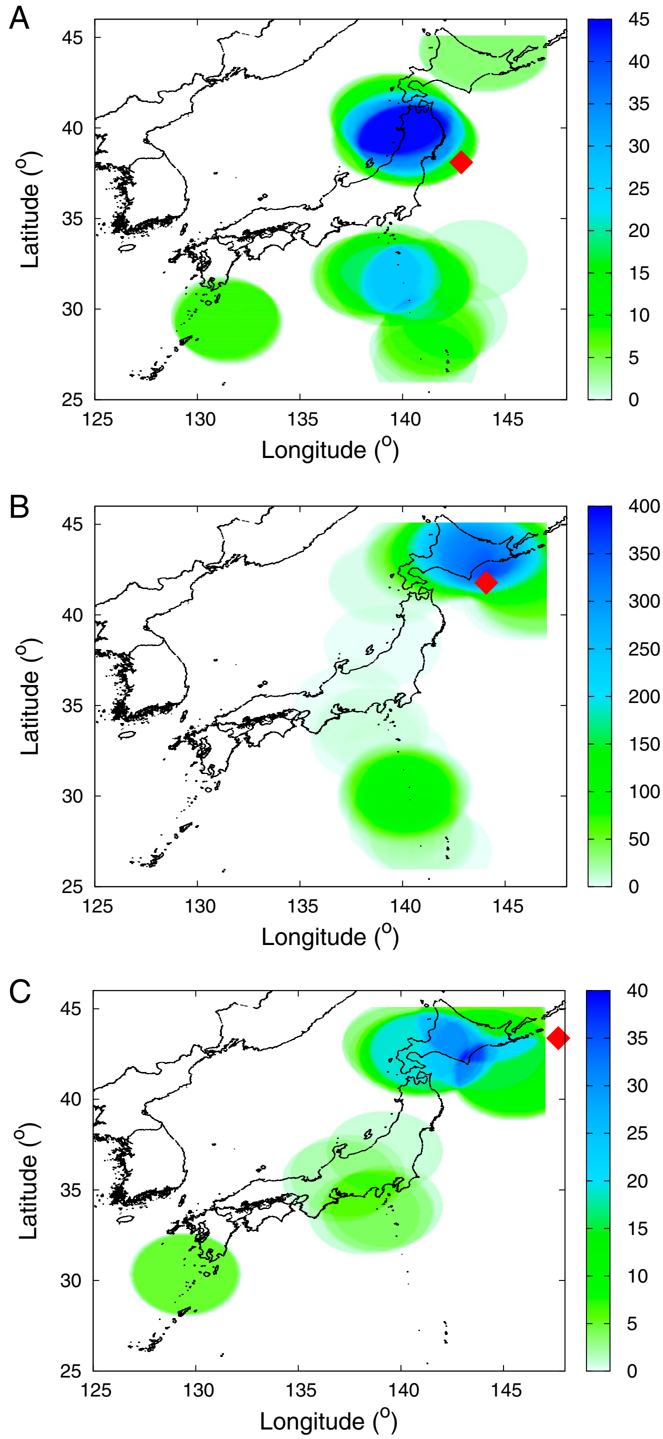

Fig. 3. Color contours of the number $n_c(x_i,y_i)$ for EQs of magnitude 8.0 or larger: (*A*) 2011 Tohoku EQ, (*B*) 2003 Off-Tokachi EQ, and (*C*) 1994 East-Off Hokkaido EQ. Solid diamonds are epicenters.

which the center is sliding through the large area with steps of 0.1° in longitude and latitude. To diminish boundary effects, the centers of small areas were restricted to lie in the region $N_{26}^{45}E_{126}^{147}$, i.e., 19° × 21°, giving rise to 191 positions along the latitude and 211 along the longitude. There were thus $191 \times 211 = 40{,}301$ small areas. However, since the distribution of epicenters is nonuniform, it was not possible to use all of them for the calculation of β. Fig. 2*B* schematically shows the distribution of the number of EQs per month in each R = 250-km small area, as deduced from the total EQ map (Fig. 2*A*), in the form of color thickness contour. For our purpose of investigating the variation of β minima in a few preseismic periods, it is necessary to determine the value of β in small areas ("local" β minimum) for every few days. To have enough number of EQs, we must have at least one event for every few days and hence no less than two

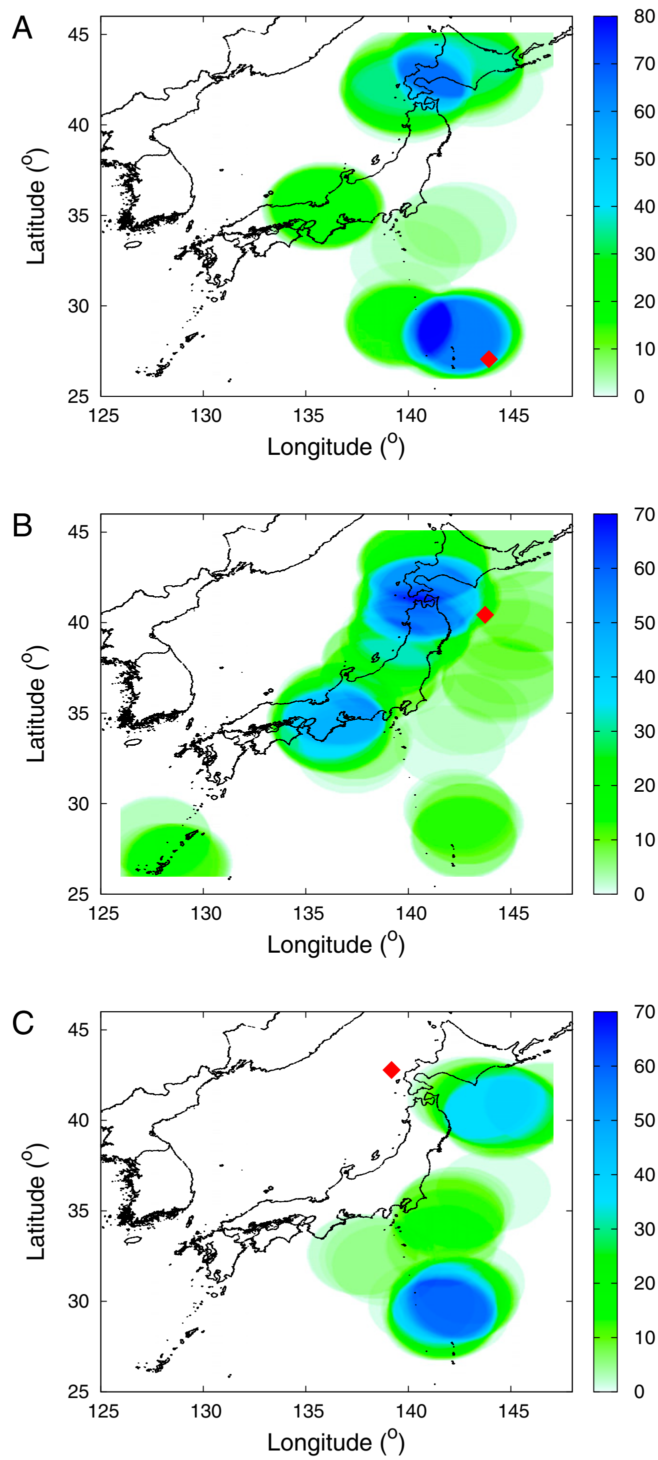

Fig. 4. Color contours of the number $n_c(x_i,y_i)$ for EQs of magnitude between 7.6 and 8.0: (*A*) 2010 Near Chichi-jima EQ, (*B*) 1994 Far-Off Sanriku EQ, and (*C*) 1993 Southwest-Off Hokkaido EQ.

events per week on average, i.e., at least eight events per month. If we impose the condition that the EQ numbers per month must be at least eight, we are left with 12,476 small areas, the W values of which are shown in Fig. 2*C*. We worked on the time changes of β for these areas. From the small areas that showed "local" β minimum, we selected the ones where the date of β minimum coincided (i.e., ± 2 d) with the one in the large area. We started our investigation at 5.5 mo before each major EQ. The reason for this was that 5.5 mo is the maximum lead time of SES activities observed to date. To assure that a "local" β minimum is clearly recognizable, we imposed the criterion that it should differ more than 10% from the β value of the events that occurred within 10 d before and after.

When "local" β minima appeared simultaneously (± 2 d) with the β minima in the large area in many small areas, we investigated the spatial distribution of their centers as follows: We counted how many of their centers lie within 250 km from each point (x_i,y_i) of a 0.05° × 0.05° grid. This number will be hereafter labeled $n_c(x_i,y_i)$. It is our aim to find out where the largest number of $n_c(x_i,y_i)$ is observed and examine whether it lies close to the epicenter of the forthcoming main shock.

Results

The above procedure has been applied for all six shallow EQs with M larger than 7.6 during the 27-y period. The results for these EQs can be visualized in Figs. 3 *A–C* and 4 *A–C*. In each case, the actual epicenter is depicted with a red diamond.

Fig. 3 *A–C* depicts the results for the three EQs of $M \geq 8$, i.e., (Fig. 3*A*) the Tohoku M9.0 EQ, (Fig. 3*B*) the Off-Tokachi M8.0 EQ on 26 September 2003, and (Fig. 3*C*) the East-Off Hokkaido M8.2 EQ on 4 October 1994. The color contours show the number $n_c(x_i,y_i)$. The results do not differ neither by changing the step of the sliding area window (bin coarseness) from 0.1° to 0.05° nor by starting investigation at 3.5 mo (instead of 5.5 mo) before EQ. Fig. 3 *A–C* shows that in all three cases, the actual epicenter was close to the area exhibiting the largest number of $n_c(x_i,y_i)$.

By the same token, Fig. 4 *A–C* depicts the results for the three EQs of magnitude between M7.6 and M8.0, i.e., (Fig. 4*A*) the Near Chichi-jima M7.8 EQ on 22 December 2010, (Fig. 4*B*) the Far-Off Sanriku M7.6 EQ on 28 December 1994, and (Fig. 4*C*) the Southwest-off Hokkaido M7.8 EQ on 12 July 1993. Concerning the first two EQs, the results are similar to those in Fig. 3 *A–C*. However, the third EQ (Fig. 4*C*) shows that the epicenter was close not to the area with the largest but to the area with the second-largest number of $n_c(x_i,y_i)$.

Conclusion

We found that, for all of the six shallow EQs of magnitude larger than 7.6 that occurred in Japan from 1 January 1984 to 11 March 2011, a large number of small areas exhibited β minimum almost simultaneously with the large area. Such small areas are accumulated in a region that lies within a few hundred kilometers of the actual epicenter. These results suggest that assessing β minimum in small areas every few days may help prelocate the epicenter of the forthcoming main shock. The present method has the benefit that it can be applied when geoelectrical data are not available, although its accuracy is less than that based on SES data.

1. Sarlis NV, et al. (2013) Minimum of the order parameter fluctuations of seismicity before major earthquakes in Japan. *Proc Natl Acad Sci USA* 110(34):13734–13738.
2. Varotsos PA, Sarlis NV, Tanaka HK, Skordas ES (2005) Similarity of fluctuations in correlated systems: The case of seismicity. *Phys Rev E Stat Nonlin Soft Matter Phys* 72(4 Pt 1):041103.
3. Varotsos P, Sarlis NV, Skordas ES, Uyeda S, Kamogawa M (2011) Natural time analysis of critical phenomena. *Proc Natl Acad Sci USA* 108(28):11361–11364.
4. Varotsos P, Lazaridou M (1991) Latest aspects of earthquake prediction in Greece based on seismic electric signals. *Tectonophysics* 188(3-4):321–347.
5. Varotsos P, Alexopoulos K, Lazaridou M (1993) Latest aspects of earthquake prediction in Greece based on seismic electric signals, II. *Tectonophysics* 224(1-3):1–37.
6. Sarlis N, Skordas E, Lazaridou M, Varotsos P (2008) Investigation of seismicity after the initiation of a seismic electric signal activity until the main shock. *Proc Jpn Acad Ser. B* 84(8):331–343.
7. Uyeda S, Kamogawa M (2008) The prediction of two large earthquakes in Greece. *Eos Trans AGU* 89(39):363.
8. Uyeda S, Kamogawa M, Tanaka H (2009) Analysis of electrical activity and seismicity in the natural time domain for the volcanic-seismic swarm activity in 2000 in the Izu Island region, Japan. *J Geophys Res* 114(B2):B02310.
9. Sarlis NV, Skordas ES, Varotsos PA (2010) Order parameter fluctuations of seismicity in natural time before and after mainshocks. *EPL* 91:59001.